Thin Solid Films 636 (2017) 602–607

Contents lists available at ScienceDirect

Thin Solid Films

journal homepage: www.elsevier.com/locate/tsf

Elucidation of the pore size and temperature dependence of the oxygen diffusion into porous silicon

Ali Gelir [a,*], Onder Yargi [b], Sureyya Aydın Yuksel [b]

[a] Department of Physics, Istanbul Technical University, 34469 Istanbul, Turkey
[b] Department of Physics, Yildiz Technical University, 34220 Istanbul, Turkey

ARTICLE INFO

Article history:
Received 31 March 2017
Received in revised form 1 June 2017
Accepted 3 July 2017
Available online 04 July 2017

Keywords:
Photoluminescence
Quenching
Porous silicon
Oxygen diffusion

ABSTRACT

Steady state photoluminescence technique is proposed for the measurement of the diffusion of oxygen into porous silicon (PS). In this work, the PS layers on *n*-type Si substrates were prepared by anodic etching in hydrofluoric (HF) acidic solution at a *dc* current under white light illumination. The PS layers with three different pore sizes (0.7, 1.9, and 4.5 μm) were obtained by etching in different HF concentrations in ethanol (from 33% to 67%). The effect of the pore size on the oxygen diffusion was performed at room temperature. In addition to the pore size, the effect of the temperature on the oxygen diffusion was also studied at 35, 45, and 65 °C for PS layer with 1.9 μm pore size. It was observed that the diffusion of the oxygen to PS layers takes place in two different stages. In the first stage, the oxygen molecules are adsorbed on the surface of the PS layer while they diffuse through into the pores in the second stage. For all cases the diffusion in the first stage is much faster than the second stage. The oxygen diffusion increases as the pore size and the temperature increase in the first stage. In the second stage, while the diffusion increases with the pore size, it almost does not change with temperature.

© 2017 Elsevier B.V. All rights reserved.

1. Introduction

Porous silicon (PS) has become the object of research due to the presence of micro- and nanocrystallites, whose sizes vary from units of nanometers to tenths of microns, on its surface [1]. PS has been divided into three categories based on the size of its pores; macro porous (larger than 50 nm), mesoporous (2 to 50 nm), and micro porous (less than 2 nm). PS has some interesting features due to its distinctive properties such as the large surface area-to-volume ratio, different pore geometry, morphology and biocompatibility [2–4].

PS shows photoluminescence (PL) property which was first observed by L.T. Canham in 1990 [5]. Although the discussions on the mechanism of the PL of PS still continue, two main explanations are used to describe the PL mechanism of PS: the quantum confinement of the charge carriers in nano-sized crystal structures of PS and Si═O bonds on the surface and in the pores of PS [6–8]. The surface modifications with different materials, such as nanocrystals, metals, and organic molecules also affect the PL character of PS [9–13]. The PL property of PS structures makes it potential material for the applications in Si based optoelectronic technology [14–20].

Diffusion of different gases, especially molecular oxygen, through the PS structure is an important phenomenon especially for the sensor and the electrical applications. Since its surface to volume ratio is very big, the chemical stability of the PS structure is low and it can be oxidized easily [21]. The oxidation as a result of diffusion of oxygen increases the resistance of the optoelectronic circuit elements and decreases the efficiency of the optoelectronic devices [22]. Different studies were performed in literature to carry out the diffusion and the effect of the oxygen on the PS structure, i.e., the interaction of the diffused oxygen with PS structure with different chemical composition [23], photosensitization of singlet oxygen generation [24], and microstructural change of the PS layers upon oxidation [21].

Quenching the PL of the PS structure is one of the main experimental techniques to observe the oxygen diffusion through the PS layer, and it was shown that the quenching obeys Stern-Volmer kinetics and mostly reversible process. The proposed mechanism for the quenching for this system is the energy transfer to molecular oxygen (O_2) adsorbed on the PS surface by the excitons in PS which results in formation of a singlet oxygen [23–25]. But this mechanism is valid only for freshly prepared PS and if the surface of the PS is covered with a barrier-like oxide, the oxygen molecules cannot quench the PL emission of PS [6]. In this case, PS must be kept in the pressured nitrogen atmosphere before the quenching experiments to replace the oxygens in the bonds on the surface of PS with the nitrogen. After the replacement oxygen with nitrogen, the quenching effect is observed again.

* Corresponding author.
E-mail address: gelira@itu.edu.tr (A. Gelir).

http://dx.doi.org/10.1016/j.tsf.2017.07.007
0040-6090/© 2017 Elsevier B.V. All rights reserved.

In this work, oxygen diffusion into PS was studied as a function of the temperature and the pore size. A model was developed on the PL quenching of PS to measure the oxygen diffusion coefficient, *D*. In this approach, it is assumed that the diffused oxygen molecules, which are the quenchers, were distributed homogeneously over the porous surface of PS. To be able to calculate the diffusion coefficients, the quenching is accurately described by a linear Stern-Volmer equation. By fitting the PL intensity versus time profile to linear Stern-Volmer equation, the diffusion coefficients were obtained depending on the pore size and the temperature. The results showed that the diffusion processes take place in two different stages. It was observed that the increasing pore size increase the diffusion coefficients at each stage. In addition, the diffusion coefficients with increasing temperature also increase at the first stage but at the second stage the values are almost the same.

2. Experimental

The PS layers on antimony doped *n*-type mono crystalline wafers Si (111) substrates with resistivity $1 \times 10^{-2}\ \Omega$ cm were prepared by anodic etching in hydrofluoric acid (HF):ethanol (EtOH) electrolyte at a *dc* current of about 15 mA cm^{-2} and under white light illumination. The Si substrates were cleaned before etching process with methanol and acetone, respectively. In this process, we used a conventional Teflon etching cell to put silicon wafer as anode and platinum wire as cathode horizontally in the HF:EtOH electrolyte and the growth of micro-pores is produced by the application of current. We changed the electrolyte concentration (33%–67%) to obtain PS films with different porosity. The etching was carried out at room condition. Finally, the PS films were rinsed in ethanol and air-dried after the process. The surface morphology of the PS layers was taken using JEOL 6335F JSM SEM scanning probe microscope at the operating voltage of 15 kV.

The diffusion experiments were performed in the cuvette holder of the fluorescence spectrophotometer. The PS layers were kept in a sealed quartz cuvette under the nitrogen environment for about 10 min and then the cap of the cuvette was opened for the oxygen diffusion to the PS layer. The PL data were collected in time drive mode during the diffusion by using Varian Carry Eclipse model fluorescence spectrophotometer. The excitation wavelengths for the PS layers with different pore sizes, 0.7, 1.9, and 4.5 μm, were set to 350, 380, and 409 nm, respectively. Also the emission wavelengths which were monitored during the time drive mode were set to 605, 597, and 603 nm depending on the pore sizes, respectively. The temperature dependence of the diffusion of the oxygen to the PS layer was performed in the temperature controlled cuvette holder of the fluorescence spectrophotometer at 35, 45 and 65 °C. For this study, a PS layer with pore size of 1.9 μm was used and the excitation and the emission wavelengths were set to 380 nm and 597 nm, respectively.

2.1. Analysis of the oxygen diffusion

The quantitative analysis of the oxygen diffusion was carried out by using Stern-Volmer kinetics and the Fickian Diffusion model. The detailed information about these models is given in the following paragraphs.

2.1.1. Stern-Volmer kinetics

When samples with photoluminescence probes are exposed to air, they are saturated with oxygen, and thus the photoluminescence emission intensities of the samples decrease due to the oxygen quenching of the excited photoluminescence probe. The mechanism of quenching involves a sequence of spin allowed internal conversion processes which takes place within a weakly associated encounter complex between the probe and the oxygen. The product is either a singlet ground state or an excited triplet state probe [26,27].

Data generated from the oxygen quenching studies of the photoluminescence probes in homogeneous environment are usually analyzed by using the Stern-Volmer relation given below, provided that the oxygen concentration $[O_2]$ is not too high [28].

$$\frac{I_0}{I} = 1 + k_q \tau_0 [O_2] \tag{1}$$

In this equation, I and I_0 are the PL intensities in the presence and absence of the oxygen, respectively, k_q is the bimolecular quenching rate constant, $[O_2]$ is the molar concentration of O_2 and τ_0 is the PL lifetime in the absence of O_2.

This equation requires that the decay of PL is single exponential and, moreover, that quenching interactions occur with a unique rate constant k_q. From the slope of a plot of I_0/I versus $[O_2]$, k_q can be determined provided that τ_0 is known.

2.1.2. Fickian diffusion

Fick's second law of diffusion was used to model diffusion phenomena in plane sheet. The following equation is obtained by assuming a constant diffusion coefficient for concentration changes in time [29].

$$\frac{C}{C_0} = \frac{x}{d} + \frac{2}{\pi} \sum_{n=1}^{\infty} \frac{\cos n\pi}{n} \sin \frac{n\pi x}{d} \exp\left(-\frac{Dn^2\pi^2 t}{d^2}\right) \tag{2}$$

where d is the thickness of the slab, D is the diffusion coefficient of the diffusant, and C_0 and C are the concentrations of the diffusant at time zero and t, respectively. x corresponds to the distance at which C is measured.

We can replace the concentration terms directly with the amount of diffusant, M, by using the following relation:

$$M = \int_v C dV \tag{3}$$

when Eq. (3) is considered for a volume element in the plane sheet and substituted in Eq. (2), the following equation is obtained [29]:

$$\frac{M_t}{M_\infty} = 1 - \frac{8}{\pi^2} \sum_{n=0}^{\infty} \frac{1}{(2n+1)^2} \exp\left(-\frac{D(2n+1)^2\pi^2 t}{d^2}\right) \tag{4}$$

where M_t and M_∞ represent the amounts of diffusant entering the plane sheet at time t and infinity, respectively.

In the present study the diffusant is oxygen molecule and according to the Eq. (1) the amount of the oxygen is directly proportional to the PL intensity [27]. Therefore, the Fick's law given in Eq. (4) for $n = 0$ can be written in terms of the photoluminescence intensity as following,

$$\frac{I_t}{I_0} = A + \frac{8C}{\pi^2} \exp\left(-\frac{D\pi^2 t}{d^2}\right) \tag{5}$$

where $C = \frac{k_q \pi_0 O_2(\infty)}{V}$ and $A = 1 - c$ (c is the value of the intensity ratio given in Eq. (5) for t goes to infinity). Here $O_2(\infty)$ is the amount of oxygen molecules diffused into latex film at time infinity.

This model is fitted to the experimental data and the diffusion coefficients (D) can be calculated by using a linear least-squares method.

3. Results and discussion

Scanning electron microscopy (SEM) analysis was carried out on the PS/Si structures, to study their surface morphology. Fig. 1 shows SEM images of the PS/Si structures. From the top view of the SEM micrograph it is evident that the sponge like surface of PS layer is homogeneous. The SEM images of the PS layer surfaces with different average pore sizes, 0.7, 1.9, and 4.5 μm, are represented in Fig. 1, respectively. In the images the bright islands and relatively dark regions are the tops of silicon walls

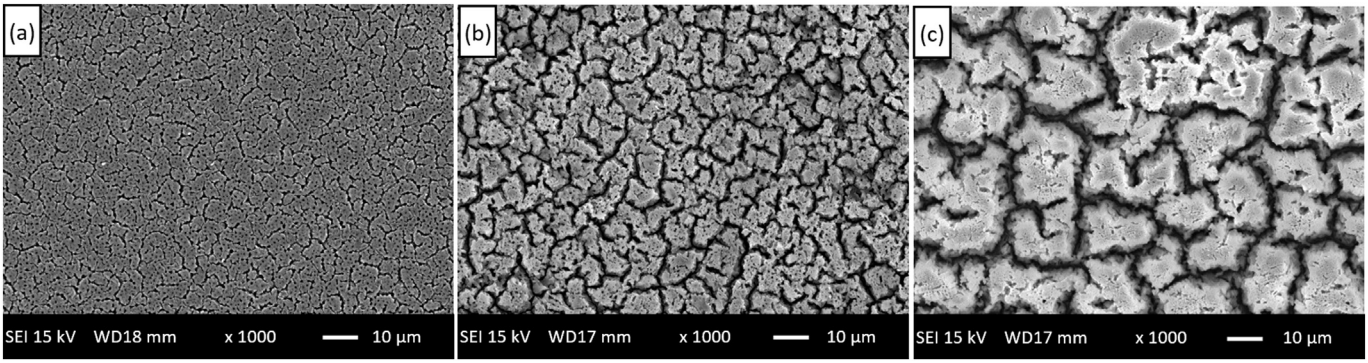


Fig. 1. SEM micrographs of the porous silicon (PS) layers with different pore sizes, (a) 0.7, (b) 1.9, and (c) 4.5 μm, respectively.

and interval empties of the porous silicon, respectively. As seen from this figure that the average pore sizes and the porosity were increased depending on the increasing HF concentration in electrolyte.

The PL spectra of PS with pore sizes, 0.7 μm, 1.9 μm and 4.5 μm, were given in Fig. 2. The following points can be concluded from this figure: *i.* the maximum wavelengths of PL emission of PS samples are in the range of 595–605 nm. This shows that the PL emission is mainly coming from the Si═O bonds in the barrier like oxide layer on the surface of PS as described in detail in reference [6]. This emission is not due to the quantum confinement of the charge carriers in the crystallites on the surface of PS layer because it is known that the PL emission wavelength coming from the Si nanocrystals in PS depends on the pore size of PS [30]. But, as seen in Fig. 2 the maximum wavelength of the PL emission is not changing with the pore size. *ii.* The emission intensity is increasing with the increasing pore size. This may be due to the increasing surface area which is excited as the pore size increases and since the excited area is increased, the emission intensity also will be increased as seen in this figure. *iii.* An additional emission peak at around 560 nm was observed for PS with highest pore size, 4.5 μm, which corresponds to the emission of the thin oxide/hydroxide layer on the PS surface [6]. This layer may be formed due to the diffusion of the water molecules in air through the wide pores of the PS sample [6].

When a freshly prepared PS layer is directly open to the air, the PL emission intensity is quenched by the oxygen molecules in air. But, the PS samples which are waited for a long time in room conditions, a barrier like oxide layer forms on the surface of PS and the oxygen in air cannot quench the PL emission of PS [6]. In this case, PS must be kept in the pressured nitrogen atmosphere before the quenching experiments to replace the oxygens in the bonds on the surface of PS with the nitrogen. In Fig. 3, the variation of the PL emission intensity at maximum wavelength with respect to time for different pore sizes were given. These measurements were performed in the cuvette holder of the spectrophotometer under a pressured nitrogen atmosphere. Here, it is clearly seen that the PL emission intensity increasing as the oxygen molecules are replaced by the nitrogen molecules as discussed above. In addition, the time to reach the saturation is shorter for PS with smaller pore size. When the pore size increased, the oxygen molecules both on the surface and in the pores are replaced during this process. But, for the smaller pore sizes probably only the oxygen molecules on the planar surface of PS are replaced.

After the replacement the oxygen with nitrogen, the quenching effect of the oxygen molecules can be observed again. The quenching experiments in this study were performed taking into account this important point and the results of the quenching experiments were represented in Fig. 4. The variations of the maximum intensities of the PL spectra given in Fig. 2 for the PS layers with different pore sizes were represented in Fig. 4(a) with respect to the diffusion time in normalized form. In addition, the results of the temperature dependence of the oxygen diffusion for the PS layer with 1.9 μm pore size were given in Fig. 4(b). It is clearly seen that as the oxygen diffused through into the planar PS layer, the emission intensity decreased according to Eq. (1) for all cases. In other words, the oxygen quenches the PL emission of PS by the mechanism mentioned in the section of Stern-Volmer kinetics.

The results of the fitting the experimental data to Eq. (5) with both single and double exponential forms were given in Fig. 5 for PS layer with 0.7 μm as an example. Here, it is clearly seen that the best fit for

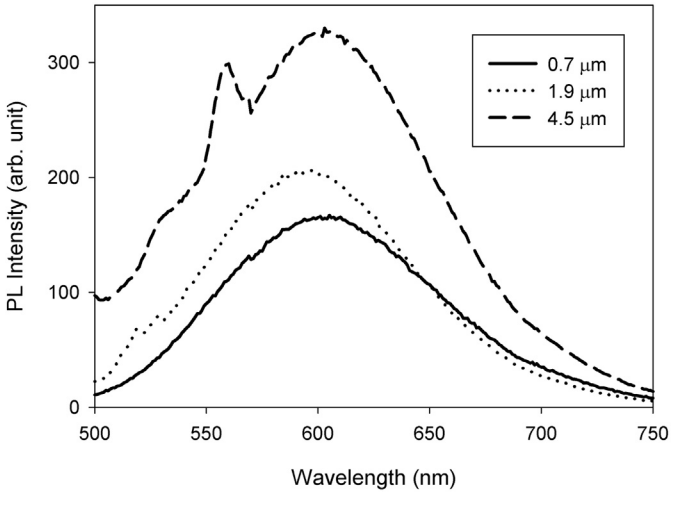


Fig. 2. The PL spectra of the PS layers with different pore sizes.

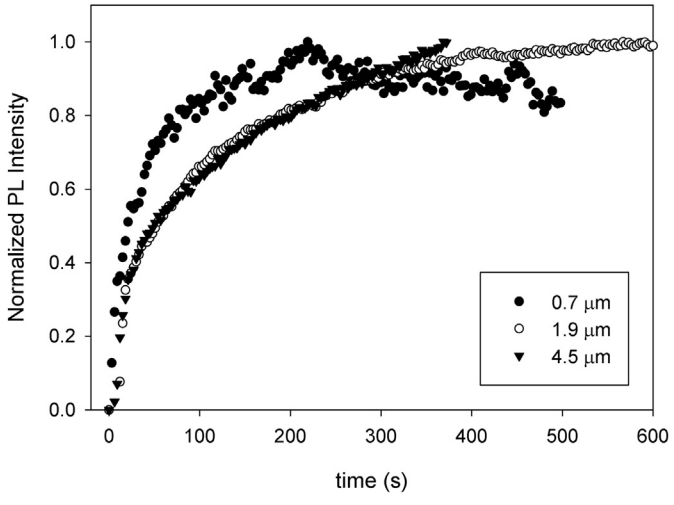


Fig. 3. Change in the PL intensity of the PS layers kept under the nitrogen environment. Each symbol in the plot shows different pore size.

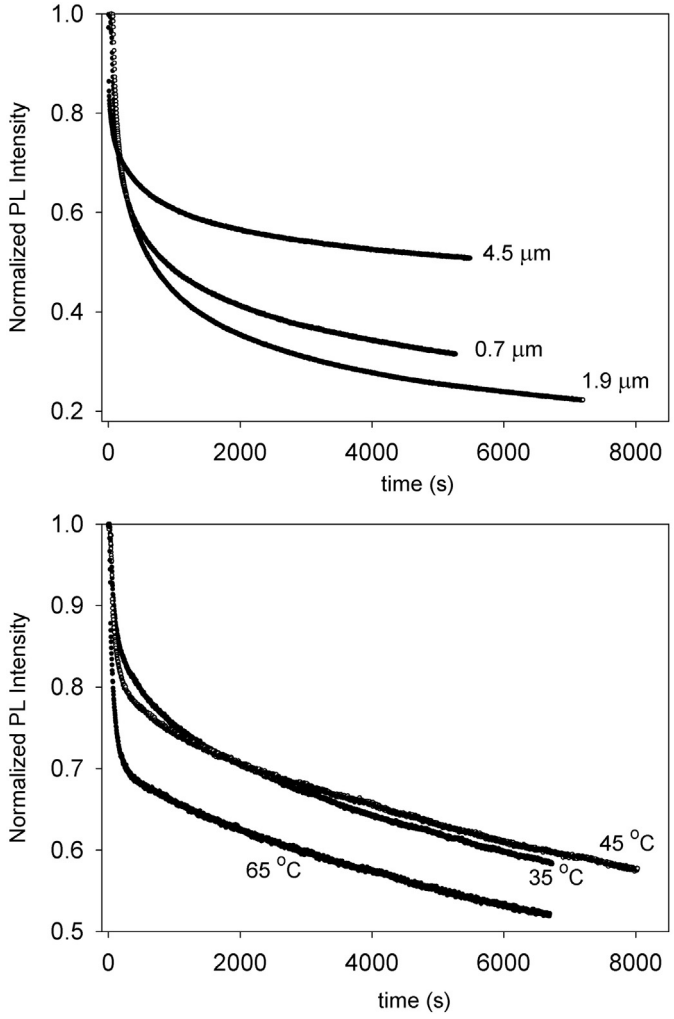


Fig. 4. Change in the PL intensity of the PS layers with different pore sizes during oxygen diffusion at room temperature (a) and at different temperatures (b) for PS layer with pore size of 1.9 μm.

the experimental data is double exponential decay form. This indicates that the diffusion of the oxygen through the PS takes place in two different stages. In the first stage, oxygen interacts with the Si atoms near the surface and the oxygen molecules are adsorbed at the surface of PS layer. In the second stage, the oxygen enters the pores and interacts with the Si atoms near the walls of the pores.

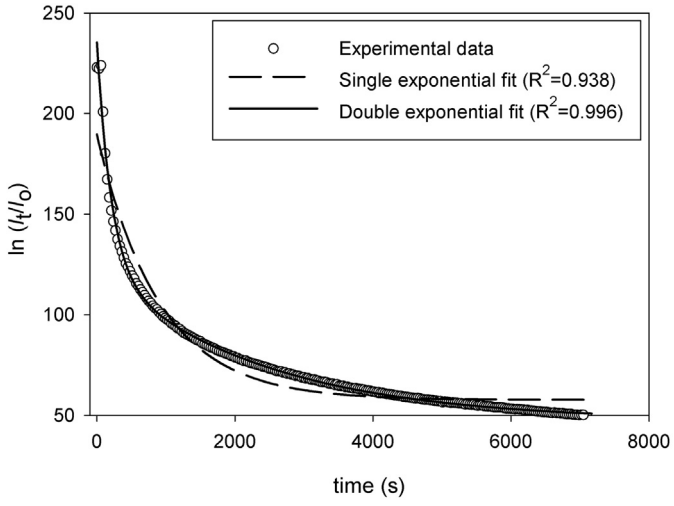


Fig. 5. The results of the fitting the experimental data to Eq. (5) with both single and double exponential forms for PS layer with 0.7 μm.

Table 1
Experimentally obtained diffusion coefficients (D) and quenching rate constants (k_q) for different pore sizes of PS.

Thickness (μm)	Porous size (μm)	$D_1 \times 10^{-11}$ ($cm^2 \cdot s^{-1}$)	$D_2 \times 10^{-11}$ ($cm^2 \cdot s^{-1}$)	$k_q \times 10^4$ ($M^{-1} \cdot s^{-1}$)
8.5	0.7	54.2	3.7	1.5
10	1.9	52.7	4.1	1.7
8.9	4.5	89.1	4.8	2.7

The calculated D and k_q values depending on the pore size are listed in Table 1 and represented in Fig. 6. The reproducibility of the results was evaluated by performing five measurements per sample. As seen from the Table 1 and Fig. 6, the diffusion coefficients of oxygen, D, are strongly dependent on the pore size. In Stage 1, the diffusion coefficient did not vary considerably for the small pore sizes. But, when the pore size increased to 4.5 μm, the diffusion coefficient also increased considerably. This may be due to the increasing surface area with increasing pore size as seen from Fig. 1, i.e., when the pore size increases, the surface area through which the oxygen molecules will diffuse increases and this will cause to obtain comparably bigger diffusion coefficients with respect to the smaller pore sizes. In Stage 2, the diffusion coefficient

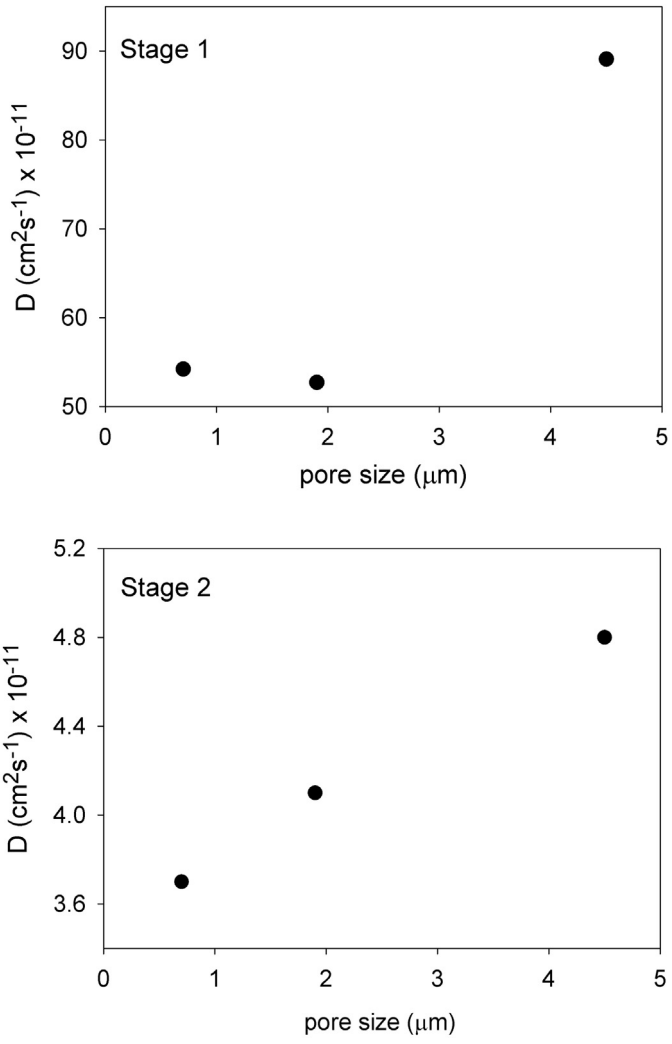


Fig. 6. Plot of the diffusion coefficients, D, versus with pore sizes at Stage 1 (a) and at Stage 2 (b).

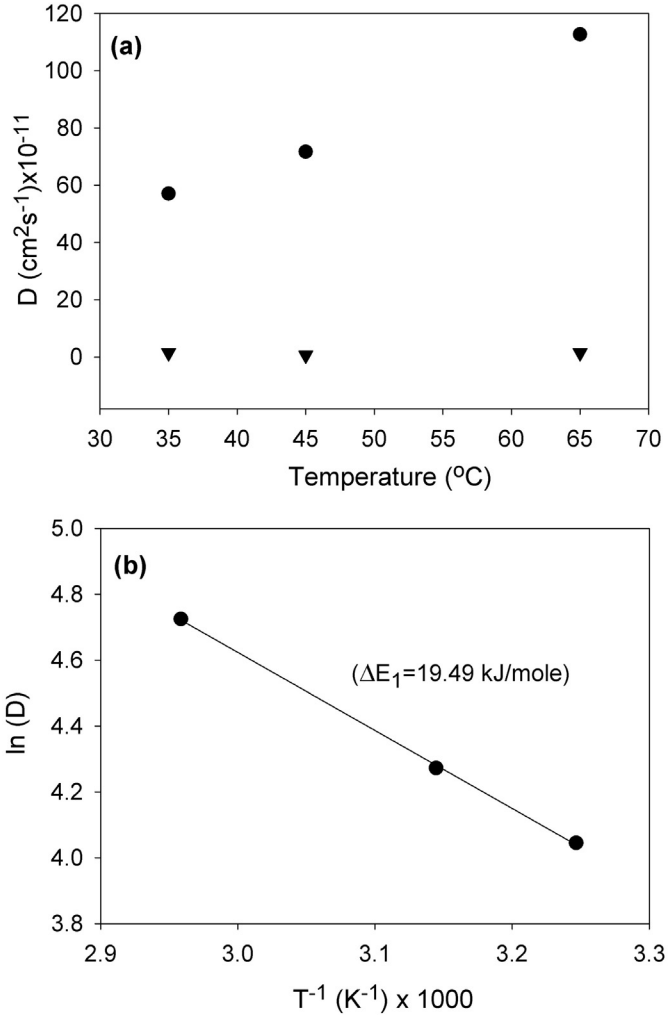


Fig. 7. Plot of the temperature dependence of diffusion coefficients (a) and the required energies for the diffusion of oxygen through the PS layer (b) for PS layer with pore size of 1.9 μm. The symbols (●) and (▼) show the Stages 1 and 2, respectively.

increases proportional to the increasing pore size. This is expected result since as the pore size increases the oxygen molecules can diffuse easier through into the pores. When we compare the diffusion coefficients of Stages 1 and 2, it is clearly seen that the diffusion coefficients in Stage 1 are bigger than those in Stage 2. This result is in consistent with the expectations. Because, less energy is required for the adsorption of the oxygen molecules on the surface of PS layer. On the other hand, the energy for the diffusion of the oxygen molecules through into the pores should be comparably bigger than the adsorption on the surface.

D values versus temperature are plotted in Fig. 7(a) and given in Table 2. As seen from Fig. 7(a), *D* values are strongly dependent on the temperature for PS especially in the Stage 1. In this stage, the oxygen molecules are adsorbed on the surface of the PS layer and this adsorption increases with the increasing temperature. This is due to the increasing Brownian motion of the oxygen molecules with the temperature which causes an increase in the probability of interaction of the oxygen molecules with the Si atoms on the surface of the PS layer. In Stage 2, the diffusion coefficient is almost constant with temperature. In this stage, since the temperature is not enough to change the pore sizes of the PS layers, it is not expected to observe a considerable change in the diffusion coefficients in this limited range of temperature.

Table 2
Experimentally obtained diffusion coefficients (D) and quenching rate constants (k_q) for different temperatures of PS with pore size of 1.9 μm.

T (°C)	$D_1 \times 10^{-11}$ (cm^2·s^{-1})	$D_2 \times 10^{-11}$ (cm^2·s^{-1})	$k_q \times 10^4$ (M^{-1}·s^{-1})
35	57.1	1.5	1.8
45	71.7	0.7	1.3
65	113.7	1.5	1.9

The diffusion of small molecules through membranes can be described as a thermally activated process that obeys Arrhenius behavior. The temperature dependence of the diffusion coefficient, *D*, can be written as follows:

$$D = D_0 \exp(-\Delta E_D / k_b T) \quad (6)$$

The required energy for the diffusion of the oxygen molecules in Stage 1 is represented in Fig. 7(b). The energy, 4.14 kJ/mole, calculated in Stage 2 is not physically meaningful because the temperature range used in this study is not enough to change the pore sizes. Therefore, only some fluctuations in the diffusion coefficients were observed depending on the temperature instead of a stable change in Stage 2.

4. Conclusion

In this study, it has been shown that the diffusion of the oxygen molecules through PS layers depends on pore size and the temperature. The PL emission mostly coming from the Si═O bonds on the PS layer. Since the samples were waited in the standard room conditions, a barrier like oxide layer formed on the surface of PS, and only the energy levels belong to Si═O bonds can be excited in this case. The diffusion of the oxygen through PS layer takes place in two different stages. In the first stage, the oxygen molecules interact with the Si atoms on the surface and in the second stage they interact with Si atoms in the pores. Pore size of the PS layer affect the diffusion of oxygen considerably in each stage, i.e., when the pore size increases, the diffusion coefficients also increase.

The diffusion coefficients in Stage 1 strongly depends on the temperature. Because, increasing temperature increases the probability of the interaction of the oxygen molecules with Si atoms. In Stage 2, since the temperature range is not enough to change the pore sizes, almost no effect of the temperature on the diffusion has been observed.

Acknowledgement

We thank to Assoc. Prof. Dr. Kenen Koç in Physics Department of Yildiz Technical University for his valuable support to our study.

References

[1] B.M. Kostishko, Y.S. Nagornov, S.V. Appolonov, The modification of the properties of n-type conductivity porous silicon by argon ion irradiation, Vacuum 73 (2004) 105–108.
[2] T. Kumeria, A. Santos, D. Losic, Nanoporous anodic alumina platforms: engineered surface chemistry and structure for optical sensing applications, Sensors 14 (2014) 11878–11918.
[3] I. Levitsky, Porous silicon structures as optical gas sensors, Sensors 15 (2015) 19968–19991.
[4] L.T. Canham, Bioactive silicon structure fabrication through nanoetching techniques, Adv. Mater. 7 (1995) 1033–1037.
[5] L.T. Canham, Silicon quantum wire array fabrication by electrochemical and chemical dissolution of wafers, Appl. Phys. Lett. 57 (1990) 1046–1048.
[6] M. Balaguer, E. Matveeva, Quenching of porous silicon photoluminescence by molecular oxygen and dependence of this phenomenon on storing media and method of preparation of pSi photosensitizer, J. Nanopart. Res. 12 (2010) 2907–2917, http://dx.doi.org/10.1007/s11051-010-9881-x.
[7] D. Kovalev, E. Gross, N. Künzner, F. Koch, V.Y. Timoshenko, M. Fujii, Resonant electronic energy transfer from excitons confined in silicon nanocrystals to oxygen molecules, Phys. Rev. Lett. 89 (2002) 137401.
[8] M.V. Wolkin, J. Jorne, P.M.M. Fauchet, G. Allan, C. Delerue, Electronic states and luminescence in porous silicon quantum dots: the role of oxygen, Phys. Rev. Lett. 82 (1999) 197–200.
[9] I. Haddadi, S. Ben Amor, R. Bousbih, S. El Whibi, A. Bardaoui, W. Dimassi, H. Ezzaouia, Metal deposition on porous silicon by immersion plating to improve photoluminescence properties, J. Lumin. 173 (2016) 257–262.

[10] M. Mizuhata, Y. Mineyama, H. Maki, Fabrication of ZnS/porous silicon composite and its enhancement of photoluminescence, Electrochim. Acta 201 (2016) 86–95.
[11] V.B. Shevchenko, O. Dacenko, V. Makara, S.L. Golovynskyi, I. Golovynska, Photoluminescence of porous silicon as an indicator of its interaction with nucleic acids, Eur. Phys. J. Appl. Phys. 76 (2016) 30401.
[12] D. Kovalev, H. Heckler, G. Polisski, F. Koch, Optical properties of Si nanocrystals, Phys. Status Solidi B 215 (1999) 871–932.
[13] C. Delerue, G. Allan, M. Lannoo, Electron-phonon coupling and optical transitions for indirect-gap semiconductor nanocrystals, Phys. Rev. B 64 (2001) 193402.
[14] R.J. Martin-Palma, R. Guerrero-Lemus, J.D. Moreno, J.M. Martines-Duart, A. Grass, D. Levy, Development and characterization of porous silicon based photodiodes, Mater. Sci. Eng. B 69–70 (2000) 87–91.
[15] R.J. Martin-Palma, L. Vazquez, J.M. Herrero, J.M. Martinez-Duart, M. Schnell, S. Schaefer, Morphological, optical and electrical characterization of antireflective porous silicon coatings for solar cells, Opt. Mater. 17 (2001) 75–78.
[16] R.J. Martin-Palma, J.M. Matinez-Duart, L. Li, R.A. Levy, Electrical behavior of double-sided metal/porous silicon structures for optoelectronic devices, Mater. Sci. Eng. C 19 (2002) 359–362.
[17] J.M. Martinez-Duart, R.J. Martin-Palma, Photodetectors and solar cells based on porous silicon, Phys. Status Solidi B 232 (2002) 81–88.
[18] H.A. Hadi, R.A. Ismail, N.F. Habubi, Optoelectronic properties of porous silicon heterojunction photodetector, Indian J. Phys. 88 (2014) 59–63.
[19] C. Wang, B. Hu, H. Yi, The study of structure and optoelectronic properties of ZnS and ZnO films on porous silicon substrates, Optik 123 (2012) 1040–1043.
[20] J. Torres, H.M. Martinez, J.E. Alfonso, L.D. López, Optoelectronic study in porous silicon thin films, Microelectron. J. 39 (2008) 482–484.
[21] R. Cisneros, H. Pfeiffer, C. Wang, Oxygen absorption in free-standing porous silicon: a structural, optical and kinetic analysis, Nanoscale Res. Lett. 5 (2010) 686–691.
[22] J. Harper, M.J. Sailor, Photoluminescence quenching and the photochemical oxidation of porous silicon by molecular oxygen, Langmuir 13 (1997) 4652–4658.
[23] D.T.J. Ee, C.K. Sheng, M.I.N. Isa, Photoluminescence of porous silicon prepared by chemical etching method, Malaysian J. Anal. Sci. 15 (2011) 227–231.
[24] M.B. Gongalsky, A.Y. Kharin, S.A. Zagorodskikh, L.A. Osminkina, V.Y. Timoshenko, Photosensitized generation of singlet oxygen in porous silicon studied by simultaneous measurements of luminescence of nanocrystals and oxygen molecules, J. Appl. Phys. 110 (2011) 13707.
[25] S. Green, P. Kathirgamanathan, The quenching of porous silicon photoluminescence by gaseous oxygen, Thin Solid Films 374 (2000) 98–102.
[26] J.B. Birks, Organic Molecular Photophysics, J. Wiley, London, New York, 1975.
[27] B. Valeur, Molecular Fluorescence: Principles and Applications, Wiley-VCH Verlag, 2001.
[28] S.A. Rice, Diffusion-Limited Reactions, Elsevier Science, 1985.
[29] J. Crank, The Mathematics of Diffusion, Oxford University Press, 2004.
[30] P. Kumar, Effect of silicon crystal size on photoluminescence appearance in porous silicon, ISRN Nanotechnol. 2011 (2011) 1–6, http://dx.doi.org/10.5402/2011/163168.